

AperTO - Archivio Istituzionale Open Access dell'Università di Torino

**Technical-economic feasibility of CHP systems in large hospitals through the Energy Hub method:  
The case of Cagliari AOB**

**This is a pre print version of the following article:**

*Original Citation:*

*Availability:*

This version is available <http://hdl.handle.net/2318/1633021> since 2020-06-03T18:05:52Z

*Published version:*

DOI:10.1016/j.enbuild.2017.04.047

*Terms of use:*

Open Access

Anyone can freely access the full text of works made available as "Open Access". Works made available under a Creative Commons license can be used according to the terms and conditions of said license. Use of all other works requires consent of the right holder (author or publisher) if not exempted from copyright protection by the applicable law.

(Article begins on next page)



# UNIVERSITÀ DEGLI STUDI DI TORINO

***This is an author version of the contribution published on:***

*Energy and Buildings, volume 147, 2017,  
doi.org/10.1016/j.enbuild.2017.04.047*

*A. Biglia, F. V. Caredda, E. Fabrizio, M. Filippi, N. Mandas*

*Volume 147, Elsevier, 2017, pag. 101 - 112*

***The definitive version is available at:***

<http://www.sciencedirect.com/science/article/pii/S0378778816310520>

# Technical-economic feasibility of CHP systems in large hospitals through the Energy Hub method: The case of Cagliari AOB

## Abstract

Multi-energy systems satisfy different energy uses of a building such as space heating, space cooling, DHW, etc. by using different energy converters and energy sources simultaneously. These systems, if properly designed and operated, have high efficiency in the production of energy.

This paper presents a method based on the Energy Hub model for the energy and economic analysis of a large hospital complex placed in Sardinia (Italy). The Energy Hub model allows dynamic simulations results and experimental data to be coupled. First of all, the model was calibrated according to real data and information obtained during an energy audit carried out by the University of Cagliari in collaboration with the Brotzu Hospital staff. Then, since cogeneration is recognised as one of the most effective ways to convert energy efficiently, the integration of a CHP system (internal combustion engine), within the multi-energy system of the hospital, was studied. The results obtained are useful to identify benefits that might be obtained by the CHP system, depending on its regulation and on the economic variables.

The presented model represents a valuable tool to evaluate possible energy and economic savings and to design and to optimise every kind of multi-energy systems of a generic building.

Keywords: Multi-energy systems; Energy Hub modelling; Large hospital; Calibration; CHP; Optimisation

## 1. Introduction

The use of energy for heating, cooling and ventilation of buildings [1] has nowadays a significant effect on the total balance of the primary energy demand in industrialised countries, and its cost has risen in the past years. Whereas energy costs are increased, inefficient energy systems are no longer acceptable and suitable. In recent decades, several actions to increase energy efficiency of buildings were proposed by researchers [2]-[9]. In particular, very effective actions were focused on improving the thermal insulation of buildings [10]-[14], increasing the efficiency and optimising the operations of HVAC systems [15]-[18], installation of more efficient energy converters such as condensing boilers, cogenerators, heat pumps, etc. [19]-[22], installation of solar thermal and PV panels and construction of passive and nZEB buildings [23]-[26]. Moreover, in order to achieve an optimal regulation of the energy converters to guarantee high level of performance in terms of energy consumption and thermal comfort, monitoring systems [27]-[30] should be adopted and installed in energy plants.

Large buildings, such as hotels, supermarkets, hospitals, schools, etc. consume a lot of energy since different services (for example space heating and cooling, ventilation system, lighting, electrical energy for refrigerators, etc.) have to be fulfilled and provided during the entire year. In particular, hospitals have a continuous electricity, heating and cooling energy demand because thermal comfort, air quality levels and specialised services for the patients have to be guaranteed without interruptions to avoid discomfort. As a result, hospitals present a great potential for energy and cost savings because the simultaneous demand of energy uses for the entire year allows several actions for energy efficiency improvement to be studied and planned.

There are many opportunities for increasing energy efficiency in hospital buildings and Čongradac et al. [31]-[32] have identified two types of methods for energy savings: subsystem or room level methods and building-level methods. In the first type of methods, measures that reduce the final energy consumption

are considered (e.g. installation of presence or temperature detectors in the rooms). On the other hand, in building-level methods, possible solutions to reduce the primary energy consumption of the building are considered (e.g. condensation boilers, heat pumps, cogeneration systems, renewable energy systems etc.). Also Buonomano et al. [33] have underlined as economic and energy savings for hospitals can be achieved by adopting different kinds of measures such as CHP systems, thermal insulation, air-cooled chillers with centrifugal compressors, new ventilation strategies and more efficient technologies (heat recovery units and variable air ventilation), etc. In particular, the authors have analysed different energy measures (roofs thermal insulation, installation of substation climatic 3-way valves and of thermostatic valves and air handling regulation) for improving energy efficiency of some buildings of a hospital, by coupling simulation tools (EnergyPlus and TRNSYS) and experimental data. Ascione et al. [34] have proposed a novel methodology to identify robust cost-optimal energy retrofit solutions; multi-stage and multi-objective optimisations were performed by coupling EnergyPlus and Matlab®.

Cogeneration systems (internal combustion engines, turbines, ORC cycles, etc.) are known to be one of the most effective solutions to reduce the energy consumptions in hospitals [35]. Compared to other plants for thermal and electrical energy production, cogeneration systems normally yield economic advantages, allowing also a significant reduction of greenhouse gas emissions. Renedo et al. [36] have showed how the sizing and the control strategy of cogenerators have a strong influence on the system economy of hospital buildings. Moreover, the authors have compared two different sizing methodologies for CHP: one based on the maximum thermal demand to maximise the electrical production and another based on the minimum thermal demand to maximise the number of hours in which the CHP system operates at nominal conditions (full load hours). Alexis and Liakos [37] have examined the financial and environmental aspects of a CHP system for an hospital in Greece and they have demonstrated that the annual energy cost can be reduced by 32.4% using a cogenerator. Gimelli and Muccillo [38] developed a methodology in order to determine the optimal configuration for a cogeneration plant in a hospital through a multi-objective approach. Indeed, the energy and financial benefits of the CHP system depend on several factors such as fuel type, economic variables and energy demand of users. Silveira et al. [39] have applied a thermo-economic analysis to evaluate a better configuration of a cogeneration plant for a university hospital.

Since dynamic energy simulations of buildings are recognised as one of the most effective ways to analyse energy consumptions and / or to identify possible energy and economic savings, the aim of this paper was to develop a mathematical model, through the methodology of the Energy Hub [40]-[45] to simulate the energy consumption of a large hospital complex. The Energy Hub is a modelling framework for complex and highly interlinked systems. This method can be used to determine the best possible scenarios, from both the economic and energy use points of view, depending on the characteristics of the energy demand, of the energy converters and on the boundary conditions; thus resulting very useful during design and operational stages. The Energy Hub model was applied to a case study, the Brotzu Hospital in Cagliari (Sardinia, Italy). Real data about the energy consumption of the hospital were available, since an energy audit [46] was carried out by the energy research group of the University of Cagliari.

At first, the numerical model was calibrated to verify its reliability by comparing results of the simulations with real data monitored and reported in the energy audit. Then, an optimisation of the existing energy system of the hospital was carried out. Finally, an alternative plant configuration, which involves the use of an internal combustion engine (ICE) for cogeneration was studied. The size of the ICE was obtained through a simulation that minimises a target economic function, in order to analyse the economic feasibility and the limitations of the cogeneration plant proposed as the cost of the fuel has a significant effect on the economic balance of the CHP system.

The paper is structured as follows. The case study is described in section 2, the Energy Hub model and its application to the Brotzu Hospital is presented in section 3. Simulations are reported in section 4 (validation and calibration) and section 5 (CHP system sizing). Section 6 is dedicated to the conclusions.

## 2. The Case Study

The Brotzu Hospital (AOB) in Cagliari is one of the biggest and most important medical centre of the Sardinia region (Italy). The hospital has 572 beds and every year almost 30,000 patients are admitted to the hospital, while approximately 150,000 outpatient services are provided.

The AOB consists of two separate complexes: 1) the main one is named "St. Michael's Hospital" and opened in 1982. In this structure, a total of 20 wards and 8 different departments for diagnosis and treatment are located; 2) the second one, much smaller than the first one, hosts the blood donation centre, some clinics and an auditorium. The total occupied area, taking into account also the car park and the heliport, is about 110,000 m<sup>2</sup> (Fig. 1).

The main building (Fig. 2), object of this work, consists of a reinforced concrete block structure divided into 13 levels that include two underground floors and an upper structure. In the basement, some departments of diagnosis (Computed Tomography, Positron Emission Tomography, Magnetic Resonance Imaging, etc.) and all the technological systems are located. The upper structure consists of eleven floors where all specialist departments are placed, together with the operating rooms. The total floor surface and the total volume of the main building are equal to 78,470 m<sup>2</sup> and 274,645 m<sup>3</sup>. The net conditioned area and volume are 62,250 m<sup>2</sup> and 217,876 m<sup>3</sup> respectively.

### 2.1 Multi-energy system of the Brotzu Hospital

The multi-energy system of the Brotzu Hospital is composed by three boilers, four chillers and six transformers. The boilers are fuel oil fired as natural gas is not yet available in Sardinia. The absence of natural gas in Sardinia involves the use of fuel oil that is much more expensive than natural gas and more polluting. In particular, to limit greenhouse gas emissions into the atmosphere, a fuel oil with low sulphur (LS fuel oil) content is used (<0.3% [47]). The adopted LS fuel oil has a density of 0.945 g/ml [48] and a viscosity of 13.3°E [49]. All the electrical loads of the hospital and the chillers are supplied by the electricity purchased from the grid.

The three boilers, one as backup unit, provide the thermal energy required for space heating and DHW of the hospital (AHU, FCU, radiators, DHW production and storage tanks). Two boilers work simultaneously in winter season when the space heating demand is high, while one boiler is used when the space heating load decreases. Each boiler has a thermal capacity of 2900 kW and therefore the total installed capacity is 8700 kW.

Four chillers, capable of delivering a total cooling capacity of 5188 kW, provide the cooling energy to the AHUs and FCUs, ensuring cooling of the various departments and wards of the hospital. Condensers of the chillers are cooled by using three cooling towers.

The power supply is located in the Power Centre, where six transformers are installed to reduce the voltage from 15 kVA (medium value of the national grid) to a low voltage of 400 V. Five transformers have a power of 1000 kVA and one transformer has a power of 800 kVA, this latter is used as backup unit. The Power Centre provides electricity to the various hospital uses (e.g. medical equipment, lighting, chillers, etc.). The total electrical power installed in the AOB accounts for 3735 kW divided into: 1) 588 kW for technical services rooms (boilers room, fire system, etc.); 2) 669 kW for terminals of the heating system and AHUs; 3) 1052 kW for chillers and cooling towers and 4) 1426 kW for electro medical equipment. The most

important medical equipment lines are connected in parallel to a backup generator, a 520 kW diesel engine, which allows the medical machines to be supplied in case of electricity interruption from the grid.

## 2.2 Energy Uses of the Brotzu Hospital

The AOB energy inputs and uses were evaluated during an energy audit carried out by the University of Cagliari staff in 2012 [46] (Sardinia Regional Law 7-8-2007 n°7). The annual energy demand is approximately 20,000 MWh (1726 toe), 43% of which is LS fuel oil, while the remaining 57% is electricity. Annual costs of energy purchase is about 2800 k€, 1900 k€ of which for electricity. Heating and domestic hot water hourly loads were obtained from the data monitoring system already installed at the facility and calibrated by the University of Cagliari team, using data recorded during the period 2008-2013. Hourly cooling loads were obtained thanks to a new data acquisition system installed and calibrated by the University staff. Energy consumption data acquired were analysed and processed using a software developed in Matlab® in order to obtain the yearly, monthly and hourly load charts. Another Matlab® software was developed to correct errors occurred during data acquisition. In particular, missing data were obtained by interpolating available data. Finally, data reported in this work represent the mean value of the total set of acquired data during the energy audit.

Annual and monthly loads (heating, cooling and electricity) are very important to characterise the energy flow within the structure, while hourly loads were used as inputs to the Energy Hub model (EH-model). The EH-model was validated and calibrated by comparing the EH-model results with the data of the Brotzu Hospital bills provided to the University by the Brotzu Hospital staff. The calibrated model was also adopted to size a CHP system. The hourly energy uses data allow the transient and the peak consumption to be considered in the EH-model. This guarantees that the EH-model results take into account the operating conditions, at partial load, of the energy converters. Table 1 shows the monthly energy input and energy use, the latter was divided into domestic hot water, heating, cooling, and electricity use.

The electricity required by the main building of the AOB (for lighting, medical equipment, elevators, etc.) is equal to 9317 MWh/year. This value accounts for the 82% of the total electricity purchased from the national grid. The difference between the total purchased electricity (11376 MWh/year) and the electricity for end uses is equal to 2059 MWh/year, which corresponds to the electricity required by the chillers. The total energy supplied by the chillers for space cooling is equal to 5561 MWh/year and therefore the average chillers' EER can be estimated as 2.7. The thermal energy for DHW and space heating accounts for 2015 and 5554 MWh/year respectively. The total energy required by the boilers (LS fuel oil) is equal to 8694 MWh/year and therefore the average boilers efficiency can be estimated as 0.87.

The specific energy consumption results in 32.4 kWh/m<sup>2</sup>/year, 89.3 kWh/m<sup>2</sup>/year, 89.3 kWh/m<sup>2</sup>/year and 149.7 kWh/m<sup>2</sup>/year in case of DHW, space heating, space cooling and electricity respectively.

## 3. The Energy Hub modelling framework

The Energy Hub modelling framework can be adopted to develop a physical and mathematical model able to simulate energy consumption of a multi-energy system. The Energy Hub model (EH-model) can be divided into three sections:

- 1) The *energy inputs* that represent the set of energy sources (e.g. fossil fuels, electricity from the grid, biomass, etc.) adopted to supply the energy converters of the multi-energy system;
- 2) The *energy converters* of the multi-energy system (e.g. boiler, CHP, heat pump, chiller, etc.);
- 3) The *energy uses* that represent the set of the end-user loads (e.g. space heating, space cooling, DHW, lighting, etc.) covered by the energy converters.

Each energy converter of the set  $\{k_1, k_2, \dots, k_z\}$  is considered as a black-box supplied by one or more energy inputs and it provides one or more end-user loads.

Each energy input, expressed as power  $P$  or energy  $E$ , is identified with the subscript in and the set of the energy sources is stated by the superscript  $\{a, b, \dots, n\}$ . The energy inputs can be expressed in a vector form as

$$\mathbf{P}_{in} = [P_{in}^a, P_{in}^b, \dots, P_{in}^n]^T \quad (1)$$

Each energy use is identified with the subscript out and the set of end-user loads is expressed with the superscript  $\{\alpha, \beta, \dots, m\}$ . The energy uses can be written in a vector form as

$$\mathbf{P}_{out} = [P_{out}^\alpha, P_{out}^\beta, \dots, P_{out}^m]^T \quad (2)$$

Once the two vectors are defined, they can be coupled in matrix form as

$$\mathbf{P}_{in} = \mathbf{D} \mathbf{P}_{out} \quad (3)$$

where the size of the matrix  $\mathbf{D}$  is equal to  $(n \times m)$ . Eq. (3) can be used to evaluate the energy inputs as a function of the energy uses or in the other way around. Normally, the energy inputs are expressed depending on the energy uses.

Two fundamental aspects are taken into account in the elements  $d_{ij}$  of the matrix  $\mathbf{D}$ :

- The connection between energy converters and energy uses;
- The efficiency of the energy converters.

The first aspect can be explained by using the parameter  $\varepsilon$ , which represents the ratio between the power of the energy converter and the load required by the end-user. For example

$$\varepsilon_k^\alpha = \frac{P_k^\alpha}{P_{out}^\alpha} \quad (4)$$

is the ratio between the load  $\alpha$  supplied by the energy converter  $k$  and the total required load  $\alpha$ . If only one energy converter is used to supply the required load  $\alpha$ ,  $P_k^\alpha$  is equal to  $P_{out}^\alpha$  and  $\varepsilon_k^\alpha$  is equal to 1, otherwise  $\varepsilon_k^\alpha$  is lower than 1. The parameter  $\varepsilon$  is constrained to a maximum value of 1 and a minimum value of 0, so where two or more energy converters are adopted to supply a single energy load, the sum of the  $\varepsilon$  values, for that energy load, must be equal to 1.

The second aspect involves the efficiency of each energy converters  $\eta_k$ , which depends on the operating condition, nominal or partial load, of the converter. The efficiency can be expressed as a function of the PLR (Part Load Ratio) and of the PLF (Part Load Factor). These parameters are defined as

$$PLR = \frac{(P_k)_{pl}}{(P_k)_{nom}} \quad (5)$$

$$PLF = \frac{(\eta_k)_{pl}}{(\eta_k)_{nom}} \quad (6)$$

where  $P_k$  and  $\eta_k$  account for the power and the efficiency of the energy converter, respectively, and the subscripts pl and nom refer to partial load and nominal operating conditions.

Summarising, each element  $d_{ij}$  of the matrix  $\mathbf{D}$  can be written as

$$d_{ij} = \frac{\varepsilon_k^m}{\eta_k} \quad (7)$$

The vector  $\mathbf{P}_{out}$  is usually known (e.g. monitoring campaign, results of energy simulation, etc.) while the other factors,  $\mathbf{P}_{in}$  and  $\varepsilon$ , may be known or unknown. Parameters  $\varepsilon$  are generally adopted as unknowns of the EH-model and the use of the Eqs. (1-7) allows three technical-financial analyses to be carried out:

- 1) The simulation of the operating conditions of a multi-energy system;

- 2) The optimisation of a multi-energy system (e.g. improving the regulation, etc.);
- 3) The design of a multi-energy system.

The Ladson et al.'s [50] method for non linear problems, based on the Generalised Reduced Gradient algorithm (GRG2), was used to solve the EH-model of the presented case study in the case of optimisation. The method can be adopted when the finding of an optimum is guaranteed with continuously differentiable functions.

The methodology of the Energy Hub has been largely adopted and recognised as a robust tool in different research field like optimisation and management of energy demand for buildings, optimisation of urban smart grid, operation of district heating network, etc. [51]-[57].

### 3.1 Application to the Brotzu Hospital

The EH-model was applied to the multi-energy system of the Brotzu Hospital to evaluate the energy inputs as a function of the AOB energy uses and of the energy converters regulation. The scheme of the existing AOB multi-energy system and the relative EH-model scheme are reported in Fig. 3.

The energy inputs at the inlet (subscript in) are LS fuel oil (superscript oil) and electricity from the grid (superscript el). The considered energy converters are three equal boilers (subscript b1-b3) and four chillers (subscript ch1-ch4). The energy uses required by the AOB are thermal energy for space heating and DHW (superscript th), cooling energy for space cooling (superscript c) and electricity for the AOB main building (superscript el). The electricity from the grid is also used to supply the four chillers.

According to Eqs. (1-7) and Fig. (3), the energy inputs can be expressed as a function of the AOB energy uses, of the factors  $\epsilon$  and of the energy converters efficiency as

$$P_{in}^{oil} = \left[ \frac{\epsilon_{b1}^{th}}{\eta_{b1}} \frac{\epsilon_{b1}^{th}}{\eta_{b1}} \frac{\epsilon_{b1}^{th}}{\eta_{b1}} \right] \cdot P_{out}^{th} \quad (8)$$

$$P_{in}^{el} = \left[ \frac{\epsilon_{ch1}^c}{EER_{ch1}} \frac{\epsilon_{ch2}^c}{EER_{ch2}} \frac{\epsilon_{ch3}^c}{EER_{ch3}} \frac{\epsilon_{ch4}^c}{EER_{ch4}} \right] \cdot P_{out}^c + P_{out}^{el}$$

The length of vector  $P_{out}$  is [8760x1] as the hourly mean power of the AOB energy uses was monitored during the energy audit [46]. Unfortunately, it was not possible to monitor, hour by the hour, the electricity consumption of the chillers during the audit campaign [46]. The energy inputs  $P_{in}$  are known on the monthly base.

The EH-model results were compared to the energy audit data to calibrate the model, and to obtain the hourly electricity consumption of the chillers. Then, the EH-model was used to propose a different regulation of the energy converters installed in the AOB to verify possible reduction of the energy consumptions and finally the technical-economic feasibility of a CHP system, by using an internal combustion engine, was investigated.

### 3.2 The energy converters of the Brotzu Hospital

#### 3.2.1 Boilers

Three equal low temperature boilers are installed in the AOB and fed by LS fuel oil. One boiler is always kept in stand-by for emergency. The LS fuel oil is stored in four tanks of 25,000 litres each. The boilers produce hot water at a temperature of about 80÷85°C while the water temperature at the inlet of the boilers is around at 70÷75°C. Boilers are regulated as a function of the AOB thermal load.



The specifications of each boiler are reported in Table 2. The performance of the boilers, as a function of the PLF and of the PLR, is reported in Fig (4). The PLF evolution of the boilers can be modelled with a linear curve as

$$PLF = -0.046 \cdot PLR + 1.0458 \quad (9)$$

The performance of the boiler increases at partial load as the PLF is larger than 1 when the PLR is lower than 1.

### 3.2.2 Chillers

Four vapour compression chillers are installed in the AOB, two chillers have a centrifugal compressor and two have a screw compressor. The chillers' condensers are cooled by three evaporative towers. The cold water produced by the chillers is around at 8÷9°C while, the water returning to the chillers is at 10÷15°C, depending on the season of the year.

The nominal capacity and EER of each chiller are reported in Table 3 while the performance depending on the PLF and on the PLR is shown in Fig. 5. The PLF curve for chillers with a centrifugal compressor is modelled according to the following mathematical expression [41]

$$PLF = \frac{PLR}{0.4345 \cdot PLR^2 + 0.3286 \cdot PLR + 0.2368} \quad (10)$$

while the equation for the PLF curve for chillers with a screw compressor is [41]

$$PLF = \frac{PLR}{-0.2137 \cdot PLR^2 + 1.119 \cdot PLR + 0.1007} \quad (11)$$

Chillers with centrifugal compressor present a maximum of the PLF when the PLR is around 70÷75%. This means that, at partial load, the chillers have an efficiency greater than the nominal one. On the contrary, chillers with screw compressor have a marked drop in the performance when PLR decreases.

## 4. Dynamic simulations: Existing energy system

### 4.1 Validation and calibration of the Energy Hub model

First of all, the Energy Hub model was used to evaluate the energy inputs of the AOB multi-energy system in order to calibrate the model by comparing the simulated results with the monitored data. The regulation of the AOB energy converters, set in the simulations, was adopted according to the information obtained in the energy audit [46].

In the winter period, AOB thermal uses (space heating and DHW) is guaranteed by the simultaneously operation of two of the three installed boilers. The second boiler is switched on when the AOB thermal load exceeds 40% of the first nominal boiler capacity [46]. Only one boiler is used when the space heating demand is low or is not required.

About chillers, since the hourly electricity consumption of the chillers was not possible to be monitored during the energy audit, the chillers' regulation was supposed as reported in Table 4. The assumptions of Table 4 are based on the available data of the energy audit (e.g. number of annual working hours of each chiller). Table 4 shows the PLR values of the chillers and the order of the chillers' operation. For example, in January, chiller #4 is the first chiller used and the second one, chiller #1, is not turned on whether the AOB cooling load does not exceed 25% of the nominal capacity of chiller #4. On the contrary, if AOB cooling demand is high, chillers work simultaneously in the order indicated in Table 4. The logic sets in the simulation can be summarised as follows: 1) only one chiller is used when the cooling load is low as in the winter period; 2) more than one chiller is adopted in the spring period when space cooling load is

medium/high and 3) all the chillers are used when the cooling load is very high in summer period.

Performance of the chillers at partial load are calculated using Eqs. (10-11).

The monthly simulation results of the EH-model calibration, in comparison with the monitored data, are reported in Fig. 6. The EH-model provides a consumption of LS fuel oil and of electricity for chillers of 692 tons and 1970 MWh per year respectively, while values of the energy audit are 735 tons per year of LS fuel oil and 2060 MWh per year of electricity for chillers. Therefore, the difference between model and audit results is within 4 % (electricity consumption) to 6 % (LS fuel oil consumption). The main differences between the EH-model and the energy audit occur respectively in the winter period for boilers and in the summer period for chillers (Fig. 6). Indeed, when heating and/or cooling loads are high, energy converters operate simultaneously; this condition is complicated to simulate because the real energy converters regulation is not precisely known. However, the simulation results can be considered satisfying in relation to the complexity of the analysed plant.

## **4.2 Optimisation of the existing energy system**

A different regulation of the energy converters was studied to evaluate possible energy savings of the existing plant shown in Fig. 3.

Since the efficiency of the boilers increases at partial load (Fig. 4), the regulation of boiler #2 was modified in order to increase the number of hours in which the boilers work simultaneously at partial load with a PLR equal to 30%. This configuration provides a consumption of 683 t per year of LS fuel oil that corresponds to a reduction of 1% compared to the simulation results (692 t per year, § 4.1). The difference between the total LS fuel oil consumption is not remarkable as the boilers were installed recently and their efficiency results very high in a wide PLR ranging (Fig. 4).

A different regulation was proposed also for the chillers to provide further electricity savings. Since chiller #4 is the most efficient chiller, when the AOB cooling load is not high (e.g. winter period), only chiller #4 could be used. Then, when cooling load is larger than the nominal capacity of chiller #4, chiller #1 is turned on and the two chillers work simultaneously as their performance increases at partial load (Fig. 5). Finally, chillers #3 and #2 are used only when the cooling load is very high in summer period. The obtained results are shown in Fig. 7. The proposed regulation of chillers provides a significant energy saving (approximately 30%) as chillers were installed in the past few years in different period of time to satisfy the increasing of the AOB cooling energy demand and the actual regulation is not efficient. Indeed, using mainly chiller #4, the total electricity consumption of the chillers is reduced from 1970 MWh per year (simulation of existing system) to 1403 MWh per year (simulation of existing system with chillers operational optimisation). The difference is remarkable and it should be considered that such savings are referred to electricity, which is not primary energy. In Italy, for example, a reduction of 1 kWh of electricity corresponds to a saving of 2.18 kWh of primary energy.

## **5. Dynamic simulations: Integration of the existing plant with a CHP system**

Special needs of a hospital involve a continuous demand of thermal and electrical energy. Therefore, the use of a CHP system may be a valuable solution to reduce the annual purchase cost of the AOB energy inputs. The technical-economic feasibility of a CHP system, through the methodology of the EH-model, is presented in this section. An internal combustion engine (ICE) supplied by LS fuel oil is selected as CHP unit and the scheme of the modified AOB multi-energy system is reported in Fig. 8.

The CHP system is connected to the heating circuit and it can work simultaneously with a boiler already installed in the AOB. The electricity produced by the ICE is used to cover part of the AOB electricity load

(main building and electricity for chillers) or it is sold to the electric grid when it exceeds the AOB demand. The mathematical formulation, according to the Energy Hub methodology, of the modified AOB multi-energy system (Fig. 8) results as

$$P_{in}^{oil} = \left[ \frac{\varepsilon_{b_1}^{th}}{\eta_{b_1}} \frac{\varepsilon_{ice}^{th}}{\eta_{ice}^{th}} \right] \cdot P_{out}^{th} \quad (12)$$

$$P_{in}^{el} = \left[ \frac{\varepsilon_{ch_1}^c}{EER_{ch_1}} \frac{\varepsilon_{ch_2}^c}{EER_{ch_2}} \frac{\varepsilon_{ch_3}^c}{EER_{ch_3}} \frac{\varepsilon_{ch_4}^c}{EER_{ch_4}} \right] \cdot P_{out}^c + P_{out}^{el} - P_{ice}^{el}$$

where the energy inputs are expressed as a function of the AOB energy uses and of the specification of the energy converters.

### 5.1 Performance of the CHP system

The CHP system solution involves the use of an internal combustion engine. The nominal efficiency of the ICE, both electric and thermal, was considered constant and equal to 0.402 and 0.422 respectively. The performance curves of the ICE are represented as a function of the PLF and of the thermal PLR in Fig. 9. The electric and thermal PLF curves can be modelled by parabolic curves as

$$PLF_{el} = -0.5085 \cdot PLR_{th}^2 + 1.0181 \cdot PLR_{th} + 0.4848 \quad (13)$$

$$PLF_{th} = 0.3412 \cdot PLR_{th}^2 - 0.6832 \cdot PLR_{th} + 1.3458 \quad (14)$$

ICE curves at partial load were obtained by literature data [46]. The ICE can be regulated until a minimum thermal PLR of 40%, and the electrical and thermal PLF decreases and increases respectively when the thermal PLR decreases.

### 5.2 Regulation of the CHP system

The internal combustion engine was supposed to be regulated as a function of the AOB thermal load. The other possibility of regulation would have been as a function of the AOB electricity load but this control logic might involve an excess of heat production during summer, when the heating load is mostly due to the DHW uses. The dynamic simulation was run according to the hourly AOB thermal load, therefore the ICE distribution factor of the thermal load  $\varepsilon_{ice}^{th}$  varies hour by hour. The ICE electricity production is bound to the produced thermal energy, thus involving the constrain

$$\frac{P_{out}^{th} \cdot \varepsilon_{ice}^{th}}{\eta_{ice}^{th}} = \frac{P_{out}^{el} \cdot \varepsilon_{ice}^{el}}{\eta_{ice}^{el}} \quad (15)$$

which represents the energy input balance of the ICE during its operation.

The regulation of the ICE was set as follows

- if the AOB thermal load is greater than the nominal power of the ICE, the ICE runs at its nominal power simultaneously to the boiler

$$P_{AOB}^{th} > (P_{ice}^{th})_{nom} \rightarrow PLR_{ice}^{th} = 1 \rightarrow \varepsilon_{ice}^{th} = \frac{(P_{ice}^{th})_{nom}}{P_{AOB}^{th}} \quad (16)$$

- if the AOB thermal load ranges from the minimum to the nominal ICE power, the ICE operates at partial load

$$(P_{ice}^{th})_{min} < P_{AOB}^{th} < (P_{ice}^{th})_{nom} \rightarrow PLR_{ice}^{th} = \frac{P_{AOB}^{th}}{(P_{ice}^{th})_{nom}} \rightarrow \varepsilon_{ice}^{th} = 1 \quad (17)$$

- if the AOB thermal load is lower than the minimum ICE power, only the boiler is used to cover the AOB thermal load.

### 5.3 Optimal sizing of the CHP system

#### 5.3.1 Objective function

The size of the ICE was obtained minimising the global cost [€] of the AOB multi-energy system. According to EN 15459 the global cost  $C_G(\tau)$  as a function of the duration of the calculation  $\tau$  is defined as

$$C_G(\tau) = C_I + \sum_i \left[ \sum_{j=1}^{\tau} (C_{a,j}(i) \cdot R_d(j) \cdot \beta_x) \right] \quad (18)$$

where:

$C_I$  initial investment costs [€]

$C_{a,j}(i)$  annual cost year  $j$  for component  $i$  (including running cost and maintenance) [€/year]

$R_d(j)$  discount rate for year  $j$

$\beta_x$  price dynamic factor.

The discount rate  $R_d$  depends on the real interest rate  $R_R$  and on the year  $j$  of the considered costs:

$$R_d = \left( \frac{1}{1 + R_R} \right)^j \quad (19)$$

whit  $R_R$  equals to

$$R_R = \frac{R - R_i}{1 + R_i} \quad (20)$$

where  $R$  and  $R_i$  account for the market interest rate (5%) and the inflation rate (3%) respectively. These latter two parameters may be time dependent but here are assumed constant.

The price dynamic factor  $\beta_x$  is a function of the market interest rate  $R$ , the inflation rate  $R_i$  and the rate of development of price considered  $R_x$  (4%):

$$\beta_x = \frac{1 - \left( \frac{1 + R_x}{1 + R} \right)^{\tau}}{1 - \left( \frac{1 + R_i}{1 + R} \right)^{\tau}} \cdot \frac{(R - R_i)(1 + R_x)}{(R - R_x)(1 + R_i)} \quad (21)$$

#### 5.3.2 Application to the Brotzu Hospital

The initial investment cost  $C_I$  of the ICE was considered a function of its nominal electrical power, while the parameter  $C_I$  was not considered for boilers and chillers and as they were already installed in the Brotzu Hospital. The maintenance cost of the CHP system was considered proportional to the electricity produced by the ICE. The number of years  $\tau$  in the global cost analysis was set equal to 10 as the lifetime of the ICE. The price of the electricity purchased from the grid was divided into three different categories (F1, F2 and F3) as a function of the period of the day. The price is minimum from 11 pm to 6 am (F3, night period), while it is maximum from 8 am to 8 pm (F1, day period) and finally, from 6 am to 8 am and from 18 pm to 23 pm (F2). Two LS fuel oil prices were also considered; indeed, if the ICE guaranties a positive primary energy saving (PES) value, thus ensuring the convenience compared to the separate energy production, a share of LS fuel oil used in the ICE is subjected to a tax reduction. This share is equal to 0.221 kg of LS fuel oil per kWh of electrical energy produced by the ICE [58]. All the economic parameters and the specification of the ICE are reported in Tables 5 and 6.

#### 5.3.3 Unknown of the global cost optimisation

The nominal power of the CHP system is the unknown of the global cost optimisation (Eq. 18). In particular, as the ICE was supposed to be regulated as a function of the AOB thermal load (Eqs. 16,17), the unknown of the optimisation problem is the nominal thermal power of the ICE, expressed as

$$(P_{ice}^{th})_{nom} = P_{max}^{th} \cdot \bar{\varepsilon}_{ice}^{th} \quad (22)$$

where  $P_{max}^{th}$  is the maximum AOB thermal load and  $\bar{\varepsilon}_{ice}^{th}$  is the design thermal load distribution of the ICE. The factors  $\bar{\varepsilon}_{ice}^{th}$  and  $\varepsilon_{ice}^{th}$  differ because  $\bar{\varepsilon}_{ice}^{th}$  represents the design value, while  $\varepsilon_{ice}^{th}$  is the seasonal value and it takes into account the ICE regulation as a function of the hourly AOB thermal load. Once the value  $\bar{\varepsilon}_{ice}^{th}$  is obtained, Eqs. (15,22) allow the nominal power of the ICE to be estimated. Summarising, Eq. (18) will be minimised as a function of the parameter  $\bar{\varepsilon}_{ice}^{th}$  taking into account the multi-energy configuration (Eq. 12), the constrain expressed in Eq. (15), the regulation of the ICE shown in Eqs. (16,17) and the parameters of Tables 5 and 6. The Generalised Reduced Gradient algorithm (GRG2), described in § 3, was used to perform the optimisation analysis.

## 5.4 Discussion of the optimisation results

The value of the factor  $\bar{\varepsilon}_{ice}^{th}$  that minimise the global cost (Eq. 18) of the CHP configuration is 0.189 (Table 7). This value, according to Eq. (15), involves a factor  $\bar{\varepsilon}_{ice}^{el}$  equal to 0.134. Therefore, the factor  $\bar{\varepsilon}_{ice}^{th}$  of the boiler and  $\bar{\varepsilon}_{ice}^{th}$  of the grid are equal to 0.811 and 0.866 respectively. The optimal configuration of the AOB multi-energy system with the CHP (Fig. 8) is based on the following components:

- an internal combustion engine with an electrical and thermal power of 370 and 380 kW respectively. The ICE covers 37.8% of the heating load of the AOB and 23.4% of the electricity load of the hospital (Table 7). These values take into account also the maintenance period of the ICE. Considering only the running period of the ICE, it covers 55.9% and 30.7% of the heating and electrical demand of the AOB. The thermal and electrical cumulative curves of the AOB and of the ICE are reported in Fig 10 where it is shown that the ICE runs at nominal condition for a high number of hours;
- a boiler that provides 62.2% of the heating load of the hospital. The boiler should be sized on the 81.1% of the AOB maximum heating load (2070 kW) that would correspond to a nominal boiler capacity of 1680 kW. However, it should be noted that the boiler adopted in the simulation, really installed in the AOB, has a nominal capacity of 2900 kW, thus resulting oversized. Indeed, the seasonal PLR value is equal to 0.229 (Table 8), this means that the boiler operates on average at about 25% of its nominal capacity;
- four vapour compression chillers (§ 4.1). The chillers are used for the AOB space cooling load. The total installed capacity of the chillers (5188 kW) does not result oversized compared to the maximum space cooling load of the hospital (5134 kW).
- connection to the national grid to cover the 76.6% of the electricity load of the AOB. The maximum power required to the grid is equal to 2406 kW (86.6% of the maximum AOB electricity load).

This configuration, compared to the existing one, leads the LS fuel oil consumption to increasing (+46.9%), hence its purchase cost increases as well (+41.7%). Moreover, as the ICE produces electricity, the load from the grid and its purchase cost decrease of 23.4% and 22.9% respectively. However, the balance of the AOB running cost is positive as the CHP system allows a saving of 91,210 € per year to be reached (Table 8). The CHP configuration does not involve a reduction in the maintenance cost of the existing plant, hence the saving that the ICE allows to reach is equal to the running cost saving (91,210 €/year) minus the ICE maintenance cost (40,709 €/year), which accounts for 50,502 €/year.

The global cost after ten years, taking into account the economic parameters of Eqs. (19-21), is 26,264,884 € in case of the existing AOB plant configuration and 26,237,149 € in case of the configuration with the CHP system solution (Table 8). In the light of the financial analysis, the advantage of the installation of an ICE is weak because the two values of the global cost are quite the same. However, as the global cost of the CHP case is lower than the global cost of the existing case, the actualised payback period of the CHP investment is lower than the time period that was taken as a reference in the calculation of the global cost. The global cost of the configuration with the CHP system was plotted as a function of the design parameter  $\bar{\epsilon}_{ice}^{th}$  in Fig. 11 and its minimum value corresponds to the obtained optimal value of  $\bar{\epsilon}_{ice}^{th}$ .

## 5.5 Parametric analysis

There are many factors affecting the optimal sizing of the CHP system, for example the energy demand of the AOB, the specification of the energy converter, the economic parameters, etc. Fourteenth cases were studied to evaluate the influence of different parameters on the sizing of the CHP system:

Case 1: No tax exemption for the LS fuel oil used in the ICE;

Case 2: Use of diesel fuel to supply the ICE instead of LS fuel oil;

Cases 3 and 4: Decrease of 10% and 20% of the AOB thermal energy load;

Cases 5 and 6: Decrease of 10% and 20% of the AOB electricity load;

Cases 7 and 8: Combination of cases 3, 5 and 4, 6;

Cases 9 and 10: Increase of 10% and 20% of the AOB thermal energy load;

Cases 11 and 12: Increase of 10% and 20% of the AOB electricity load;

Cases 13 and 14: Combination of cases 9, 11 and 10, 12.

The aim of the parametric analysis in cases 3 to 14 is to verify how a theoretical AOB energy demand variation affects the CHP sizing. Therefore, it was not considered how it would be possible to reduce or increase the energy demand but just the effect on the CHP sizing. The energy converters performance and economic parameters were not modified in the parametric analysis. All the cases were compared to the optimisation results of § 5.4, considered as Case 0 and reported in Table 9 together with the parametric results.

Results of Cases 1 and 2 show as the CHP system is not economically convenient whether the LS fuel oil price is not reduced or diesel fuel is used in the ICE instead of LS fuel oil. When the AOB thermal energy demand, hypothetical decreases of 10% and 20% (Cases 3, 4, 7, 8), the nominal thermal power of the ICE, compared to Case 0, reduces of 10.3% and 23.1%. In Cases 3 and 4, the total thermal energy produced by the ICE, normalised to the total thermal energy demand of the AOB ( $\epsilon_{ice}^{th}$  in Table 9), does not modify while the  $\epsilon_{ice}^{el}$  value reduces to 0.208 (-11.1%) and to 0.182 (-22.2%). In Cases 5 and 6, the effect of the AOB electrical energy demand reduction of 10% and 20% respectively on the CHP sizing was analysed. The nominal power of the ICE does not modify in comparison with Case 0 but the  $\epsilon_{ice}^{el}$  increases to 0.261 (+11.5%) and to 0.293 (+25.2%) respectively to Case 5 and 6.

Contrarily, a hypothetical increase in the AOB thermal energy demand of 10% and 20% (Cases 9, 10, 13, 14) leads the nominal thermal power of the ICE to increasing of 12.8% and 25.6%. The  $\epsilon_{ice}^{el}$  values, compared to Case 0, increase in Cases 9 and 10 to 0.261 (+11.5%) and 0.289 (+23.5%). In Cases 11 and 12, the nominal power of ICE does not modify even if the AOB electrical load was supposed to increase of 10% and 20% respectively. However, the  $\epsilon_{ice}^{el}$  values decrease to 0.213 (-8.9%) and 0.195 (-16.7%).

In all the Cases 3 to 14, it should be noted as the design parameter  $\bar{\epsilon}_{ice}^{th}$  is within the range 0.18 - 0.20. This involves an optimal nominal thermal power of the ICE equal to about the 20% of the maximum thermal

load of the AOB. Indeed, a low value of the thermal power of the ICE, compared to the AOB maximum request, guarantees operation of the CHP at nominal efficiency for a high number of hours.

## 6. Conclusions

A numerical tool, based on the Energy Hub modelling framework, coupling dynamic simulations and experimental data, was developed in this work and applied to the multi-energy system of the Brotzu Hospital, one of the largest hospital complex in Sardinia Region (Italy).

An energy audit was carried out by the research group of the University of Cagliari in collaboration with the Brotzu Hospital staff. The energy uses of the hospital (space heating, DHW, space cooling and electricity) and the energy inputs (LS fuel oil and electricity) were identified. The obtained data were used to validate and calibrate the Energy Hub model and to perform simulations on the operation and regulation of the hospital multi-energy system. Results of the simulations and of the energy audit show that the total installed capacity of the three equal boilers is oversized compared to the peak demand of the AOB. However, specifications of the boilers allow a high value of efficiency production to be reached. On the contrary, the total capacity of the four chillers does not result oversized with respect to the maximum cooling demand of the AOB but the cooling energy production does not result very efficient. A different regulation of the chillers would allow an electrical energy saving of 600 MWh/year (§ 4.2) to be reached. This amount of saving corresponds to about 100,000 €/year and this technical action would not require several and very expensive modification to the existing building's plant.

A different plant configuration that involves the use of CHP system, an internal combustion engine supplied by LS fuel oil, was studied. The global cost of the existing AOB plant configuration and of the proposed configuration with the CHP system were evaluated and compared. The size of the ICE was determined minimising the global cost of the multi-energy system after ten years as it represents the ICE lifetime. The optimisation results showed as the two global cost are similar as the price of the LS fuel oil represents a key role in the running cost of the ICE. Indeed, the absence of natural gas in Sardinia and the high price of the LS make the CHP solution weak from an economic point of view.

The results obtained shown as the developed tool is very useful to design a multi-energy system of a complex building in order to achieve the best configuration and guarantee the best return on investment.

## Figures

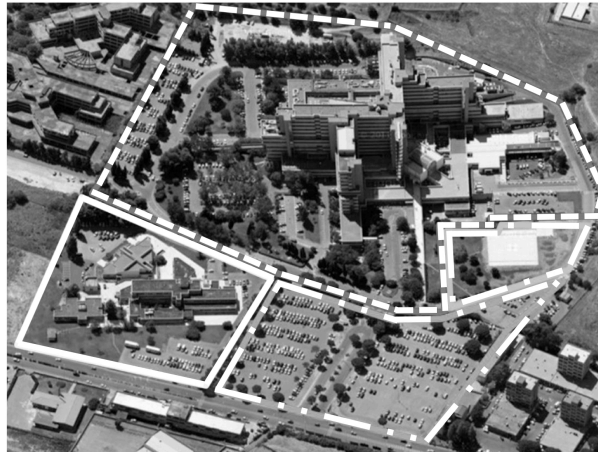


Fig. 1. Aerial view of the Brotzu Hospital. The main building and the second one are represented with dashed line and with solid line. The car park and the heliport are represented with dashed double dot line and dashed dot line respectively.



Fig. 2. Main building of the Brotzu Hospital.

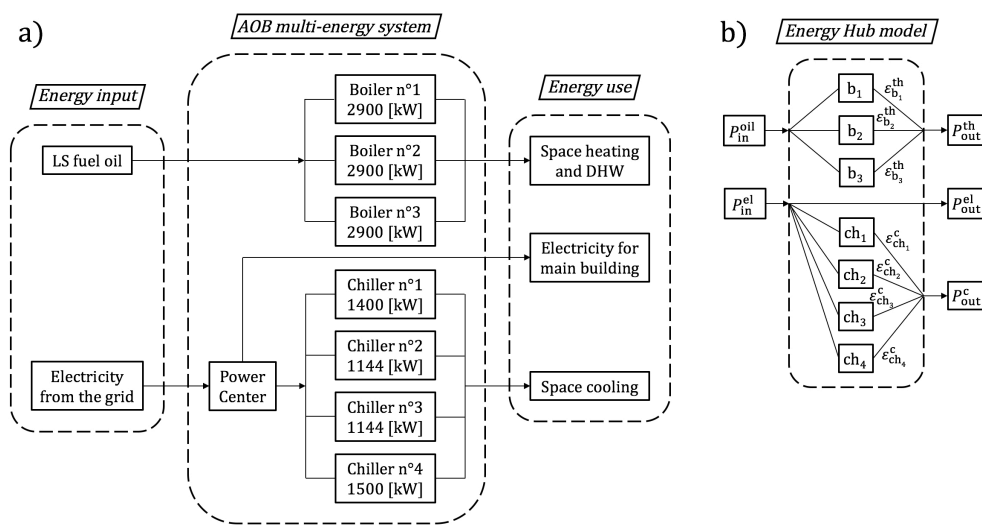


Fig. 3. Scheme of the existing AOB multi-energy system (part a) and its representation according to the Energy Hub methodology (part b).



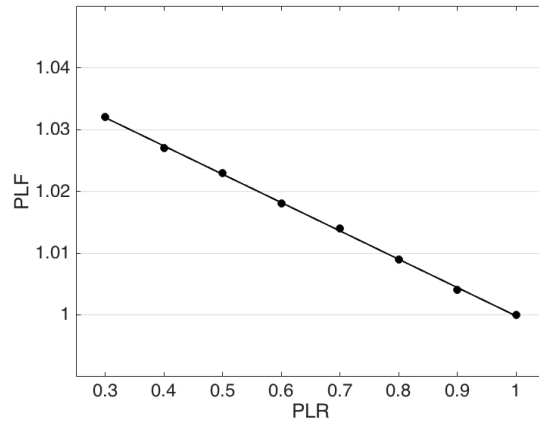


Fig. 4. PLF of the boilers as a function of the PLR. Circles represent real data sheet values while the solid line represents the interpolation curve.

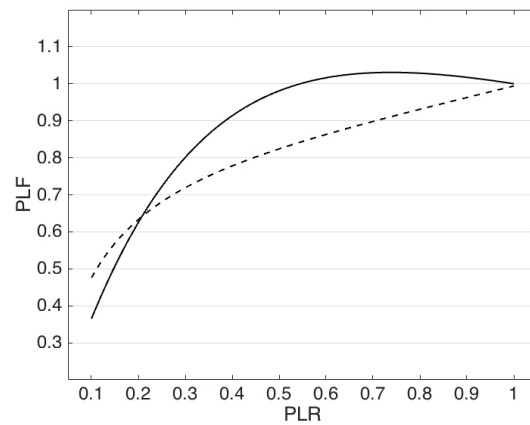


Fig. 5. PLF evolution of the chillers as a function of the PLR. Chillers with centrifugal and screw compressor are represented by solid line and dashed line respectively.

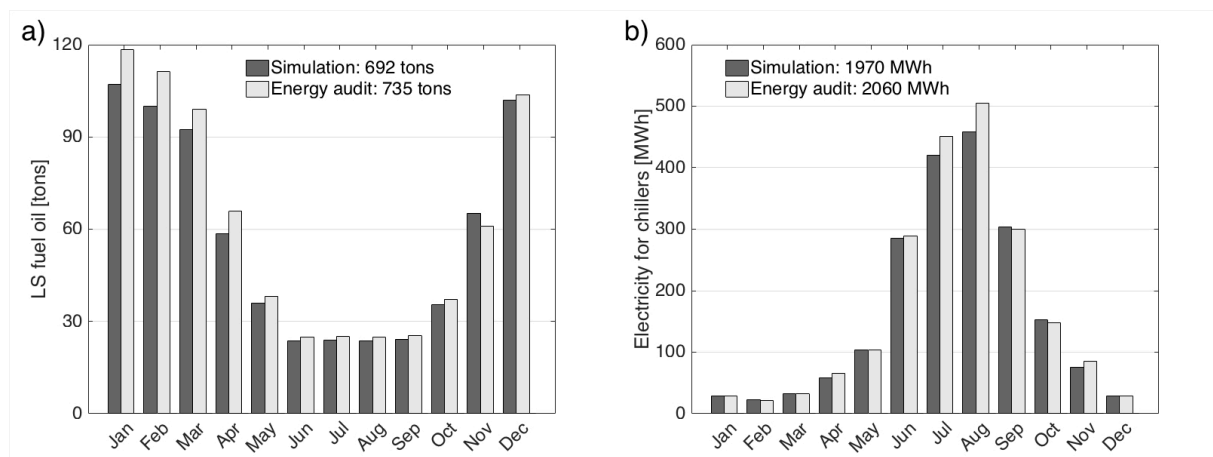


Fig. 6. Energy input consumption of LS fuel oil (part a) and of electricity for chillers (part b). Simulation results are represented by dark grey bars while results of the energy audit are reported in light grey bars.

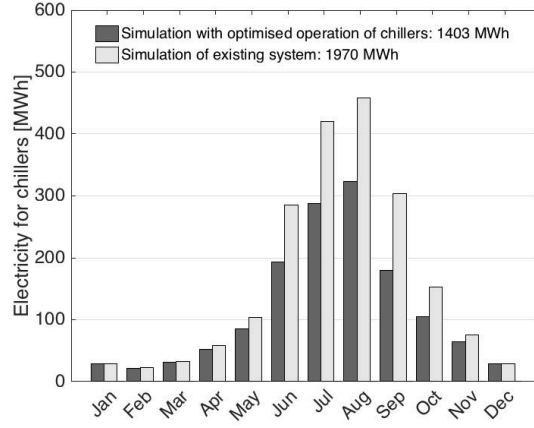


Fig. 7. Electricity consumption for chillers. Optimisation results are represented by dark grey bars while monitored data are reported in light grey bars.

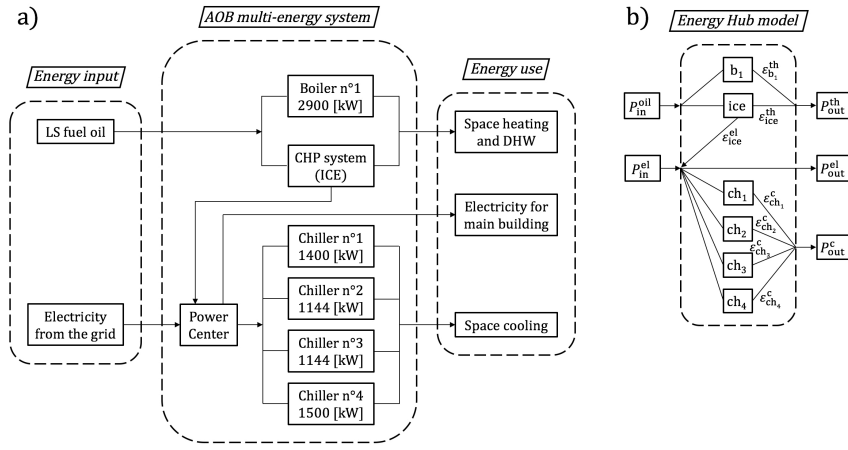


Fig. 8. Scheme of the integration of the AOB multi-energy system with the CHP system (part a) and its representation according to the Energy Hub methodology (part b).

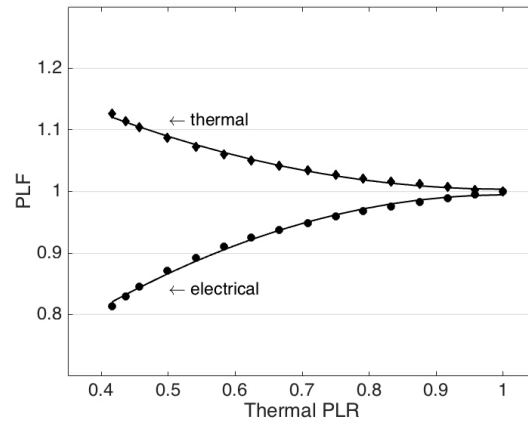


Fig. 9. PLF evolution of the ICE as a function of the thermal PLR. Circles and diamonds represent real data of the electrical and thermal PLF of the ICE and the black lines represent the interpolation curves.

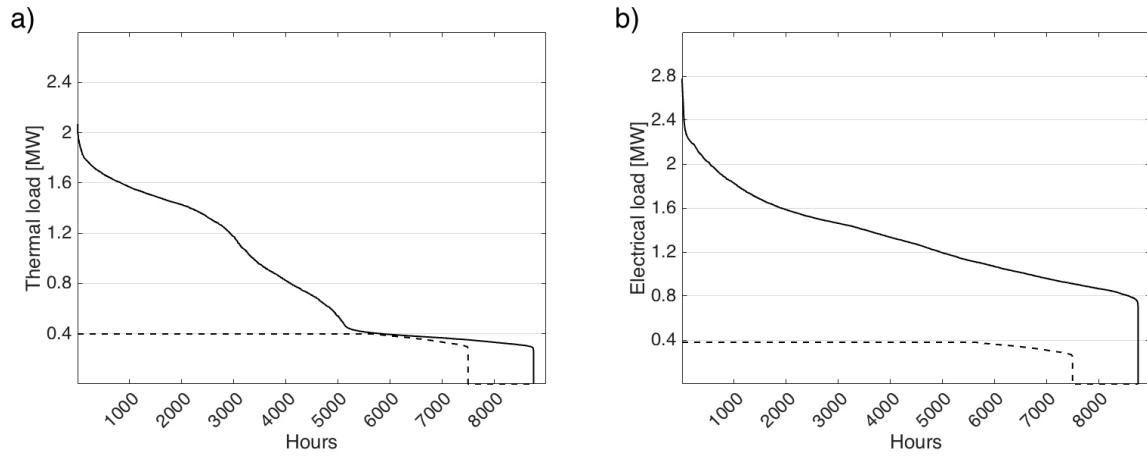


Fig. 10. Cumulative curves of the AOB and of the CHP system. Part a) refers to the thermal load while part b) refers to the electrical load. The solid line represents the AOB while the dashed line represents the CHP system.

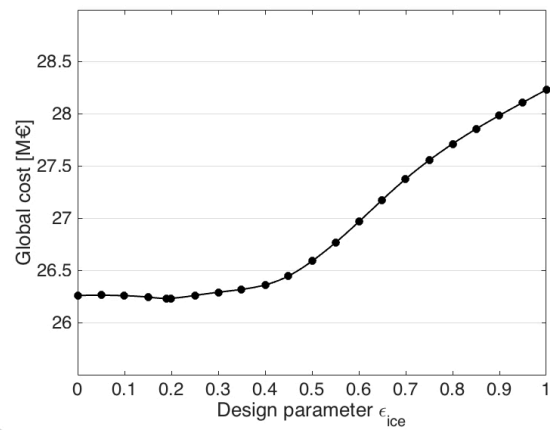


Fig. 11. Global cost of the AOB multi-energy system with the CHP system as function of the design parameter  $\epsilon_{ice}^{th}$ .

## Tables

Table 1. Monthly energy input and energy use of the Brotzu Hospital.

	Energy input (by bills)		Energy use (by monitoring)			
	Electricity from the grid	LS fuel oil	DHW	Space heating	Space cooling	Electricity for end uses
	[MWh]	[MWh]	[MWh]	[MWh]	[MWh]	[MWh]
January	830	1408	171	1065	78	801
February	758	1325	154	957	59	736
March	811	1180	171	815	87	778
April	755	783	166	513	178	689
May	864	444	171	198	281	760
June	1023	299	166	108	780	735
July	1324	306	171	106	1218	873
August	1303	300	171	94	1361	799
September	1097	309	166	98	811	797
October	946	410	171	184	400	798
November	809	695	166	457	231	724
December	856	1235	171	959	77	827
Annual	11376	8694	2015	5554	5561	9317

Table 2. Specification of the boilers.

Nominal capacity [kW]	2900
Nominal efficiency	0.925
Partial load (30%) efficiency	0.955
Max operating pressure [bar]	6
Max operating temperature [°C]	120

Table 3. Specification of the chillers.

	Chiller n°1	Chiller n°2	Chiller n°3	Chiller n°4
Nominal capacity [kW]	1400	1144	1144	1500
Nominal EER	4.53	5.50	5.50	6.08
Type of compressor	centrifugal	screw	screw	centrifugal

Table 4. Regulation of the chillers. Columns from two to five represent the PLR of the chillers while column six represents the order of chillers' operation.

	Chiller n°1	Chiller n°2	Chiller n°3	Chiller n°4	Operated order
January	0.80	0.60	0.45	0.25	4-1-3-2
February	0.80	0.60	0.45	0.25	4-1-3-2
March	0.80	0.60	0.45	0.25	4-1-3-2
April	0.70	0.60	0.30	0.30	3-4-1-2
May	0.40	0.40	0.25	0.20	4-1-3-2
June	0.30	0.25	0.20	0.20	1-4-3-2
July	0.15	0.15	0.55	0.40	4-1-3-2
August	0.15	0.15	0.55	0.55	1-4-3-2
September	0.40	0.15	0.15	0.20	4-1-3-2
October	0.65	0.35	0.45	0.20	1-3-4-2
November	0.50	0.50	0.30	0.20	4-1-3-2
December	0.80	0.70	0.55	0.30	4-1-3-2

Table 5. Specification of the ICE.

Lifetime [hours]	5000
Working hours [hours/year]	7500
Working lifetime [years]	10
Investment cost [€/kW <sub>el</sub> ]	$-0.5 \cdot P_{el} + 1400$
Maintenance cost [c€/kWh <sub>el</sub> ]	1.5

Table 6. Price of the AOB energy inputs.

LS fuel oil	[c€/kWh]	10.50
	[c€/kg]	122.3
LS fuel oil no taxes	[c€/kWh]	9.90
	[c€/kg]	114.9
Electricity	[c€/kWh]	F1: 23.02
		F2: 14.54
		F3: 11.94
		sale: 9.0

Table 7. Results of the CHP system optimisation: factors  $\varepsilon$  and PLR.

Design values	$\bar{\varepsilon}_{ice}^{th}$	0.189
	$\bar{\varepsilon}_{ice}^{el}$	0.134
	$\bar{\varepsilon}_b^{th}$	0.811
	$\bar{\varepsilon}_{grid}^{el}$	0.866
Seasonal values	$\varepsilon_{ice}^{th}$	0.378
	$\varepsilon_{ice}^{el}$	0.234
	$\varepsilon_b^{th}$	0.622
	$\varepsilon_{grid}^{el}$	0.766
Seasonal values	$PLR_{ice}^{th}$	0.977
	$PLR_{ice}^{el}$	0.973
	$PLR_b^{th}$	0.229

Table 8. Results of the CHP system optimal design: economic analysis.

LS fuel oil purchase [€/year]	existing AOB system	841,129
	AOB system with ICE	1,191,957
Electricity purchase [€/year]	existing AOB system	1,926,254
	AOB system with ICE	1,484,215
Running cost saving [€/year]		91,210
ICE investment cost [€]		451,569
ICE maintenance cost [€/year]		40,709
Global cost (Eq. 18) [€]	existing AOB system	26,264,884
	AOB system with ICE	26,237,149
Primary energy saving <sup>a</sup> [TEP/year]		135

<sup>a</sup> 2.44 and 1.35 were applied as primary energy factors for electricity and LS fuel oil

Table 9. Parametric analysis results.

	ICE size [kW]		Design values				Seasonal values			
	$P_{ice}^{el}$	$P_{ice}^{th}$	$\bar{\varepsilon}_{ice}^{th}$	$\bar{\varepsilon}_{ice}^{el}$	$\bar{\varepsilon}_b^{th}$	$\bar{\varepsilon}_{grid}^{el}$	$\varepsilon_{ice}^{th}$	$\varepsilon_{ice}^{el}$	$\varepsilon_b^{th}$	$\varepsilon_{grid}^{el}$
Case 0	370	390	0.189	0.134	0.811	0.866	0.378	0.234	0.622	0.766
Case 1	-	-	0	0	1	1	0	0	1	1
Case 2	-	-	0	0	1	1	0	0	1	1
Case 3	330	350	0.186	0.119	0.814	0.881	0.373	0.208	0.627	0.792
Case 4	290	300	0.182	0.103	0.818	0.897	0.367	0.182	0.633	0.818
Case 5	370	390	0.189	0.149	0.811	0.851	0.378	0.261	0.622	0.735
Case 6	370	390	0.189	0.168	0.811	0.832	0.378	0.293	0.622	0.707
Case 7	330	350	0.186	0.132	0.814	0.868	0.373	0.231	0.627	0.765
Case 8	290	300	0.182	0.129	0.818	0.871	0.367	0.227	0.633	0.773
Case 9	420	440	0.193	0.150	0.807	0.850	0.384	0.261	0.616	0.735
Case 10	460	490	0.196	0.167	0.804	0.833	0.390	0.289	0.610	0.711
Case 11	370	390	0.189	0.122	0.811	0.878	0.378	0.213	0.622	0.787
Case 12	370	390	0.189	0.112	0.811	0.888	0.378	0.195	0.622	0.805
Case 13	420	440	0.193	0.137	0.807	0.863	0.384	0.238	0.616	0.762
Case 14	460	490	0.196	0.139	0.804	0.861	0.390	0.241	0.610	0.755

## Nomenclature

### Symbols

AHU	Air handling unit
AOB	Brotzu Hospital of Cagliari (Sardinia, Italy)
CHP	Combined heat and power
DHW	Domestic hot water
E	Energy [kWh]
EER	Energy efficiency ratio
FCU	Fan coil unit
ICE	Internal combustion engine
LS	Low sulphur
P	Power [kW]
PES	Primary energy saving
PLF	Ratio between energy converter efficiency at partial and nominal load
PLR	Ratio between energy converter power at partial and nominal load

### Greek letters

$\varepsilon$	Distribution factor
$\eta$	Efficiency

### Subscripts and Superscript

b	Boiler
c	Cooling
ch	Chiller
ice	Internal combustion engine
el	Electrical
th	Thermal

## Acknowledgements

The energy audit carried out by the energy research group at the University of Cagliari was commissioned and funded by the Region of Sardinia through the Regional Law 7-8-2007 n°7.

## References

- [1] M. Chung, H.C. Park. Comparison of building energy demand for hotels, hospitals, and offices in Korea. *Energy* 92 (2015) 383-393.
- [2] A. Trianni, E. Cagno, A. De Donatis. A framework to characterize energy efficiency measures. *Appl Energ* 118 (2014) 207-220.
- [3] A. Allouhi, Y. El Fouih, T. Kousksou, A. Jamil, Y. Zeraouli, Y. Mourad. Energy consumption and efficiency in buildings: current status and future trends. *J Clean Prod* 109 (2015) 118-30.
- [4] A. Kyritsis, E. Mathas, D. Antonucci, M. Grottke, S. Tselepis. Energy improvement of office buildings in Southern Europe. *Energy and Buildings* 123 (2016) 17-33.
- [5] N. Aste, P. Caputo, M. Buzzetti, M. Fattore. Energy efficiency in buildings: What drives the investments? The case of Lombardy Region. *Sustainable Cities and Society* 20 (2016) 27-37.

- [6] K. Vringer, M. van Middelkoop, N. Hoogervorst. Saving energy is not easy: An impact assessment of Dutch policy to reduce the energy requirements of buildings. *Energy Policy* 93 (2016) 23-32.
- [7] A. Martínez-Molina, I. Tort-Ausina, S. Cho, J.L. Vivancos. Energy efficiency and thermal comfort in historic buildings: A review. *Renew Sust Energy Rev* 61 (2016) 70-85.
- [8] T. Wang, X. Li, P.C. Liao, D. Fang. Building energy efficiency for public hospitals and healthcare facilities in China: Barriers and drivers. *Energy* 15 (2016) 588-97.
- [9] R. Fuliotto, F. Cambuli, N. Mandas, N. Bacchin, G. Manara, Q. Chen. Experimental and numerical analysis of heat transfer and airflow on an interactive building facade. *Energy Buildings* 42 (2010) 23-28.
- [10] A. Limam, A. Zerizer, D. Quenard, H. Sallee, A. Chenak. Experimental thermal characterization of bio-based materials (Aleppo Pine wood, cork and their composites) for building insulation. *Energy Buildings* 116 (2016) 89-95.
- [11] K. Biswas, S.S. Shrestha, M.S. Bhandari, A.O. Desjarlais. Insulation materials for commercial buildings in North America: An assessment of lifetime energy and environmental impacts. *Energy Buildings* 112 (2016) 256-269.
- [12] X. Cao, J. Liu, X. Cao, Q. Li, E. Hu, F. Fan. Study of the thermal insulation properties of the glass fiber board used for interior building envelope. *Energy Buildings* 107 (2015) 49-58.
- [13] F.E. Bofo, Z. Chen, C. Li, B. Li, T. Xu. Structure of vacuum insulation panel in building system. *Energy Buildings* 85 (2014) 644-653.
- [14] W.M. Lewandowska, W. Lewandowska-Iwaniak. The external walls of a passive building: A classification and description of their thermal and optical properties. *Energy Buildings* 69 (2014) 93-102.
- [15] S. Rotger-Grifol, R.H. Jacobsen, D. Nguyen, G. Sørensen. Demand response potential of ventilation systems in residential buildings. *Energy Buildings* 121 (2016) 1-10.
- [16] P. Aparicio Ruiz, F.J. Sánchez de la Flor, J.L. Molina Felix, J. Salmerón Lissén, J. Guadix Martín. Applying the HVAC systems in an integrated optimization method for residential building's design. A case study in Spain. *Energy Buildings* 119 (2016) 74-84.
- [17] F. Ascione, N. Bianco, R.F. De Masi, G.P. Vanoli. Rehabilitation of the building envelope of hospitals: Achievable energy savings and microclimatic control on varying the HVAC systems in Mediterranean climates. *Energy Buildings* 60 (2013) 125-138.
- [18] A. Teke, O. Timur. Assessing the energy efficiency improvement potentials of HVAC systems considering economic and environmental aspects at the hospitals. *Renew Sust Energy Rev* 33 (2014) 224-235.
- [19] R.M. Lazzarin. The importance of the modulation ratio in the boilers installed in refurbished buildings. *Energy Buildings* 75 (2014) 43-50.
- [20] A.D. Smith, P.J. Mago, N. Fumo. Benefits of thermal energy storage option combined with CHP system for different commercial building types. *Sustain Energy Technol Assessments* 1 (2013) 3-12.
- [21] A.S. Ibáñez, J.I. Linares, M.M. Cledera, B.Y. Moratilla. Sizing of thermal energy storage devices for micro-cogeneration systems for the supply of domestic hot water. *Sustain Energy Technol Assessments* 5 (2014) 37-43.
- [22] G. Martinopoulos, K.T. Papakostas, A.M. Papadopoulos. Comparative analysis of various heating systems for residential buildings in Mediterranean climate. *Energy Buildings* 124 (2016) 79-87.
- [23] M. Horváth, D. Kassai-Szoó, T. Csoknyai. Solar energy potential of roofs on urban level based on building typology. *Energy Buildings* 111 (2016) 278-289.
- [24] J. Schnieders, W. Feist, L. Rongen. Passive Houses for different climate zones. *Energy Buildings* 105 (2015) 71-87.
- [25] A. Figueiredo, J. Kämpf, R. Vicente. Passive house optimization for Portugal: Overheating evaluation and energy performance. *Energy Buildings* 118 (2016) 181-196.
- [26] M. Hamdy, A.T. Nguyen, J.L.M. Hensen. A performance comparison of multi-objective optimization algorithms for solving nearly-zero-energy building design problems. *Energy Buildings* 121 (2016) 57-71.
- [27] M. Waseem Ahmad, M. Mourshed, D. Mundow, M. Sisinni, Y. Rezgui. Building energy metering and environmental monitoring – A-state-of-the-art review and directions for future research. *Energy Buildings* 120 (2016) 85-102.



- [28] A. Biglia, E. Fabrizio, M. Ferrara, P. Gay, D. Ricauda Aimonino. Performance Assessment of a Multi-energy System for a Food Industry. *Energy Procedia* 82 (2015) 540-545.
- [29] E. Fabrizio, A. Biglia, V. Branciforti, M. Filippi, S. Barbero, G. Tecco, P. Mollo, A. Molino. Monitoring of a micro-smart grid: Power consumption data of some machineries of an agro-industrial test site. *Data in Brief* 10 (2017) 564-568.
- [30] A. Costantino, E. Fabrizio, A. Biglia, P. Cornale, L. Battaglini. Energy Use for Climate Control of Animal Houses: The State of the Art in Europe. *Energy Procedia* 101 (2016) 184-191.
- [31] V. Čongradac, B. Prebiračević, N. Petrovačkić. Methods for assessing energy savings in hospitals using various control techniques. *Energy Buildings* 69 (2014) 85-92.
- [32] V. Čongradac, B. Prebiračević, B. Jorgovanović, D. Stanišić. Assessing the energy consumption for heating and cooling in hospitals. *Energy Buildings* 48 (2012) 146-154.
- [33] A. Buonomano, F. Calise, G. Ferruzzi, A. Palombo. Dynamic energy performance analysis: Case study for energy efficiency retrofits of hospital buildings. *Energy* 78 (2014) 555-572.
- [34] F. Ascione, N. Bianco, C. De Stasio, G.M. Mauro, G.P. Vanoli. Multi-stage and multi-objective optimization for retrofitting a developed hospital reference building: A new approach to assess cost-optimality. *Appl Energy* 174 (2016) 37-68.
- [35] U. Çakir, K. Çomaklı, F. Yüksel. The role of cogeneration systems in sustainability of energy. *Energy Convers Manage* 63 (2012) 196-202.
- [36] C.J. Renedo, A. Ortiz, M. Mañana, D. Silió, S. Pérez. Study of different cogeneration alternatives for a Spanish hospital center. *Energy Buildings* 38 (2006) 484-490.
- [37] G.K. Alexis, P. Liakos. A case study of a cogeneration system for a hospital in Greece. Economic and environmental impacts. *Appl Therm Eng* 54 (2013) 488-496.
- [38] A. Gimelli, M. Muccillo. Optimization criteria for cogeneration systems: Multi-objective approach and application in an hospital facility. *Appl Energy* 104 (2013) 910-923.
- [39] J.L. Silveira, W. de Queiroz Lamas, C.E. Tuna, I.A. de Castro Villela, L.S. Miro. Ecological efficiency and thermoeconomic analysis of a cogeneration system at a hospital. *Renew Sust Energy Rev* 16 (2012) 2894-2906.
- [40] M. Geidl. Integrated modeling and optimization of multi-carrier energy systems. Ph.D. thesis, Swiss Federal Institute of Technology (ETH), 2007, 124 pp.
- [41] E. Fabrizio. Modelling of multi-energy systems in buildings. *Energetica and Génie Civil* Ph.D. thesis, July 2008.
- [42] E. Fabrizio, M. Filippi, J. Virgone. An hourly modelling framework for the assessment of energy sources exploitation and energy converters selection and sizing in buildings. *Energy Buildings* 41 (2009) 1037-1050.
- [43] E. Fabrizio, M. Filippi M, J. Virgone. Trade-off between environmental and economic objectives in the optimization of multi-energy systems. *Build Simul* 2 (2009) 29-40.
- [44] E. Fabrizio. Feasibility of polygeneration in energy supply systems for health-care facilities under the Italian climate and boundary conditions. *Energy Sustain Dev* 15 (2011) 92-103.
- [45] E. Fabrizio, M. Filippi, M. Torbino. Operational optimization of actual energy systems by means of the energy hub theory. 12th Conference of Int. Building Performance Simulation Association Building Simulation, Sydney (2011) 2793-2798.
- [46] F.V. Caredda. Diagnosi Energetica dell'Azienda Ospedaliera G. Brotzu. Mechanical Design Ph.D. thesis, Cagliari, June 2013.
- [47] EN ISO 8754. Petroleum products - Determination of sulphur content - Energy-dispersive X-ray fluorescence spectrometry. CEN, European Committee for Standardization.
- [48] EN ISO 3675. Crude petroleum and liquid petroleum products - Laboratory determination of density - Hydrometer method. CEN, European Committee for Standardization.
- [49] EN ISO 3104. Petroleum products - Transparent and opaque liquids - Determination of kinematic viscosity and calculation of dynamic viscosity. CEN, European Committee for Standardization.
- [50] L.S. Ladson, A.D. Waren, A. Jain, M. Ratner. Design and testing of a generalised reduced gradient code for nonlinear programming, *ACM T. Math Software* 4 (1978) 34-50.

- [51] M. Batić, N. Tomašević, G. Beccuti, T. Demiray, S. Vraneš. Combined energy hub optimisation and demand side management for buildings. *Energy Buildings* 127 (2016) 229-241.
- [52] M. Rastegar, M. Fotuhi-Firuzabad. Load management in a residential energy hub with renewable distributed energy resources. *Energy Buildings* 107 (2015) 234-242.
- [53] F. Brahman, M. Honarmand, S. Jadid. Optimal electrical and thermal energy management of a residential energy hub, integrating demand response and energy storage system. *Energy Buildings* 90 (2015) 65-75.
- [54] T. Ma, J. Wu, L. Hao. Energy flow modeling and optimal operation analysis of the micro energy grid based on energy hub. *Energy Conversion and Management* 133 (2017) 292-306.
- [55] A. El-Zonkoly. Optimal scheduling of observable controlled islands in presence of energy hubs. *Electric Power Systems Research* 142 (2017) 141-152.
- [56] S. Pazouki, M.-R. Haghifam. Optimal planning and scheduling of energy hub in presence of wind, storage and demand response under uncertainty. *International Journal of Electrical Power* 80 (2016) 219-239.
- [57] B. Morvaj, R. Evins, J. Carmeliet. Optimising urban energy systems: Simultaneous system sizing, operation and district heating network layout. *Energy* 116 Part 1 (2016) 619-636.
- [58] Decreto Legislativo n°504/95 aggiornato dal Decreto Legislativo 2 febbraio 2007 n°26 e testo unico sulle accise.